



Impact of climate forcing on ecosystem processes in the North Pacific Subtropical Gyre

Guido Corno,^{1,2} David M. Karl,³ Matthew J. Church,³ Ricardo M. Letelier,¹ Roger Lukas,³ Robert R. Bidigare,⁴ and Mark R. Abbott¹

Received 24 May 2006; revised 27 September 2006; accepted 29 November 2006; published 26 April 2007.

[1] Measurements at the Hawaii Ocean Time-series (HOT) Station ALOHA (22°45'N, 158°W) have revealed a significant, approximately 50% increase in euphotic zone depth-integrated rates of primary production (PP; mol C fixed m⁻² d⁻¹) based on in situ ¹⁴C experiments. The character of the nearly two-decade increasing trend in PP was punctuated by several abrupt episodes that coincided with changes in the El Niño/Southern Oscillation (ENSO), and the Pacific Decadal Oscillation (PDO) climate indices, or both. In contrast to the observed increase in rates of PP, the PP per unit chlorophyll *a* (mol C fixed mol chl *a*⁻¹ d⁻¹), a measure of the biomass-normalized production, was relatively constant, whereas PP per unit solar radiation (mol C fixed mol quanta⁻¹), a measure of the efficiency of light utilization, varied in synchrony with the temporal trend in PP. Coincident with variations in PP, the HOT program core data sets also revealed changes in mixed-layer depth, upper ocean stratification, inorganic nutrients, phototrophic microbial abundances and pigment inventories. These time-series data suggest that the ENSO/PDO may control upper ocean stratification and vertical nutrient delivery into the euphotic zone at Sta. ALOHA, thereby influencing the composition of the plankton assemblage and altering rates of PP and particulate matter export.

Citation: Corno, G., D. M. Karl, M. J. Church, R. M. Letelier, R. Lukas, R. R. Bidigare, and M. R. Abbott (2007), Impact of climate forcing on ecosystem processes in the North Pacific Subtropical Gyre, *J. Geophys. Res.*, 112, C04021, doi:10.1029/2006JC003730.

1. Introduction

[2] Oligotrophic gyres represent approximately 75% of the total world oceans. Due to their vast surface area, these gyres play a significant role in solar energy capture, bioelemental cycling and carbon export [Martin *et al.*, 1987]. Thus, although rates of primary production (PP) in these areas are typically lower than in coastal or upwelling zones [Longhurst *et al.*, 1995], even small variations in PP can have a significant impact on the global oceanic carbon cycle. Recent evidence suggests that oligotrophic regions, once considered biological deserts with low ecosystem variability, demonstrate relatively high spatial and temporal variability in PP and chlorophyll *a* [Karl *et al.*, 2002; Marañon *et al.*, 2003; Wilson, 2003]. Such variations may be related to different physical forcing depending on the temporal and spatial scales over which the observations are considered [Karl *et al.*, 1995; Letelier *et al.*, 2000; Sakamoto *et al.*, 2004]. Of particular interest to constrain ocean ecosystem and geochemical models are ocean-basin scale

events that appear linked to climate variability events such as the El Niño/Southern Oscillation (ENSO) and the Pacific Decadal Oscillation (PDO).

[3] Despite chronic nutrient limitation in the upper portion (0–100 m) of the North Pacific Subtropical Gyre (NPSG), both plankton biomass and rates of PP demonstrate considerable temporal variability (variance range 20–400%) [Laws *et al.*, 1987; Karl *et al.*, 1996; Letelier *et al.*, 1996; Karl, 1999; Karl *et al.*, 2002]. Interannual variability in plankton biomass and PP has been attributed to alterations in upper ocean nutrient supply stemming from physical variations due to ENSO and PDO [Karl *et al.*, 2001, 2002]. Karl *et al.* [1995] hypothesized that ENSO events enhanced N₂-fixation by stabilizing the upper ocean and shoaling mixed layer depths (MLD) due to anomalously light winds and increased insolation (due to reduced clouds). On longer timescales, variations in the phase of the PDO may also be responsible for observed decadal changes in PP in the NPSG, as inferred by a significant increase in total chlorophyll *a* (Chl *a*) during summer months over nearly three decades [Venrick *et al.*, 1987]. The extended positive phase of the PDO during this period (1965–1977) led to a concomitant increase in winter winds, decrease in sea surface temperature (SST) and an apparent shift in the carrying capacity of the NPSG [Venrick *et al.*, 1987]. Ocean-climate related temporal variability in PP may also influence the composition of the plankton assemblages. During the PDO positive phase (1965–1977) the plankton assemblage of the NPSG appears to have shifted toward an

¹College of Oceanic and Atmospheric Sciences, Oregon State University, Corvallis, Oregon, USA.

²Now at United Nations Educational, Scientific, and Cultural Organization, Quito, Ecuador.

³School of Ocean and Earth Science and Technology, University of Hawaii, Honolulu, Hawaii, USA.

⁴The Hawaii Institute of Marine Biology, Kane'ohe, Hawaii, USA.

ecosystem dominated by prokaryotes and this transition altered food web dynamics, new and export production, nutrient supply, and fishery yields [Karl, 1999; Karl *et al.*, 2001].

[4] A formal assessment of the coherence of the NPSG response to changes in ENSO and PDO events (i.e. magnitude and synchrony) has not been presented, despite the potential significance of such coherence to elemental cycling and trophic dynamics in the ocean. Furthermore, such an analysis could provide a framework for the assessment of the resilience of the NPSG ecosystem to perturbation, and in turn, the level of self-organization for that habitat [Laws, 2003]. ENSO and PDO fluctuate on different timescales, with ENSO demonstrating higher frequency ocean-climate variability (1–3 years), while the PDO is dominated by lower frequency variability (10–30 years) [Mantua *et al.*, 1997]. Because these two climate phenomena can vary independently and exhibit variable strength in either a “warm” or “cold” phase [Mantua *et al.*, 1997; Wolter and Timlin, 1998], it is possible for phase transitions to either coincide or not, possibly resulting in fundamentally different ecosystem forcing modes. Most phase transitions appear to coincide with termination of ENSO warm events, but most ENSO warm event terminations do not coincide with PDO transitions [Graham, 1994; Barnett *et al.*, 1999]. To date, the large-scale physical interactions in the upper ocean of the NPSG occurring during and between these phase transitions remain largely unknown. The Hawaii Ocean Time-series (HOT) program provides the only existing dataset to assess temporal variability in PP in the NPSG over timescales ranging from intra-annual to subdecadal [Karl and Lukas, 1996]. In this study we analyze 17 years of monthly measurements on PP (based on in situ ^{14}C incorporation into particulate matter), picoplankton abundances (derived from flow cytometric and pigments analyses), particulate matter fluxes, nutrient concentrations, and hydrographic conditions to evaluate the response of the NPSG ecosystem to large-scale climate perturbation events.

2. Methods

2.1. Biological and Chemical Data

[5] PP, particulate material export (at the 150 m reference depth), nutrient concentrations, flow cytometric picoplankton abundances, and pigment concentrations were measured at Station ALOHA (A Long-term Oligotrophic Habitat Assessment; $22^{\circ}45'\text{N}$, 158°W) as part of the ongoing HOT program (data available at <http://hahana.soest.hawaii.edu/hot/hot-dogs/interface.html>). Protocols used for sampling, experimentation and analysis were consistent throughout the study; they are documented elsewhere [Letelier *et al.*, 1996; Karl *et al.*, 2001].

2.2. Climate Data

[6] Temporal variability in ENSO was assessed using the Multivariate ENSO Index (MEI) (data obtained from the NOAA Climate Diagnostics Center at <http://www.cdc.noaa.gov/people/klaus.wolter/MEI/table.html>). Briefly, the MEI is calculated as the first unrotated Principal Component (PC) of six observed fields combined (sea-level pressure, zonal and meridional components of the surface wind, sea surface temperature, surface air temperature, and total cloud

cover). These observations are confined to the tropical Pacific. In order to keep the MEI consistent, all seasonal values are standardized by the seasonal variance during the 1950–93 reference period; a positive and negative MEI refer to El-Niño and La-Niña favorable conditions, respectively [Wolter and Timlin, 1998].

[7] The index of the PDO was obtained from the Joint Institute for the Study of the Atmosphere and Ocean (<http://jisao.washington.edu/pdo/PDO.latest>). Standardized values for the PDO index were derived as the leading principal component of monthly SST anomalies in the North Pacific Ocean poleward of 20°N [Mantua *et al.*, 1997]. The monthly mean global average SST anomalies are removed to separate this pattern of variability from any large-scale warming signal that may be present in the time-series data.

[8] In order to determine regional effects of ENSO and PDO at Sta. ALOHA, average sea surface heights (SSH) between the NOAA Hilo and Honolulu tide gauges ($\text{SSH}_{\text{Hi-Ho}}$) were calculated. $\text{SSH}_{\text{Hi-Ho}}$ data were obtained from the NOAA National Data Buoy Center (<http://www.ndbc.noaa.gov/Maps/Hawaii.shtml>). Variability of this regional sea level index is due to a combination of local Ekman pumping and remote forcing via Rossby waves.

[9] Time-series of the mixed layer depth (MLD) were calculated from the HOT CTD data archive as the depth where (i) an offset of 0.125 in potential density (σ_{θ}) from the surface value, and (ii) a gradient of 0.005 in $\sigma_{\theta} \text{ m}^{-1}$ occurred. Finally, time-series of the buoyancy frequency in the upper 200 m was also calculated for Sta. ALOHA, which quantifies the detailed variability of upper ocean stratification.

2.3. Statistical Analysis

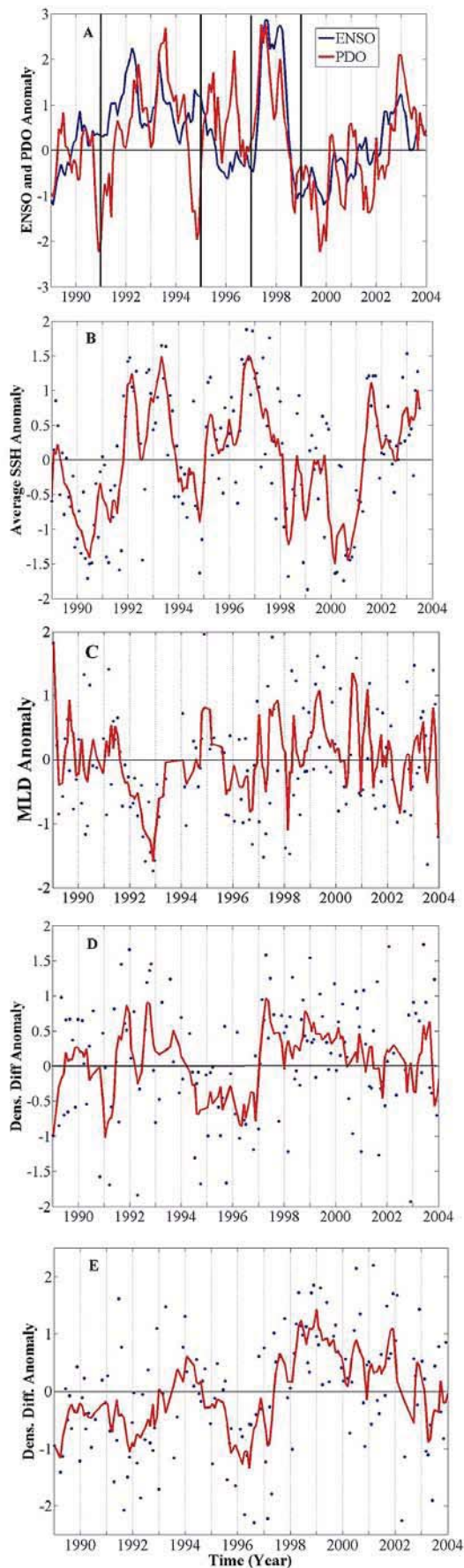
[10] Normalized anomalies (defined here as the z-score) for each variable were obtained to determine possible trends in relation to changes in ENSO, PDO and local SSH. The z-score was calculated as $z_i = (x_i - \mu)/\sigma$, where x_i is the measured value, and μ and σ are the 17-year monthly mean and standard deviation values, respectively, for all observations x_1, x_2, \dots, x_i .

[11] In order to compare differences in biogeochemical parameters to variability in ENSO and PDO indices, biogeochemical measurements made at Station ALOHA over the past 17 years were divided into 5 periods based on changes in the ENSO, PDO and SSH. After testing for normal distribution within the five periods, significant differences between periods were tested using Analysis of Variance (ANOVA), changing the significance level for each comparison according to the refined Bonferroni method [Hochberg, 1988], and t-test at 0.05 significance level.

3. Results

3.1. Physical Forcing and Habitat Response

[12] During the HOT program observation period (1989–present), the NPSG has had two relatively strong positive (warm) ENSO forcing events. The first event occurred between 1991–1994 and the second event, which was larger in magnitude, occurred during 1997–1998 (Figure 1a). The PDO index exhibited variability similar to the MEI during 1991–1994 and 1997–1998 events, but



the PDO index was in a positive phase during 1995–1996, while the MEI index was negative (Figure 1a). Three negative (cold) events also occurred during 1988, 1996 and 1998–2001. Monthly anomalies of the SSH averages between Hilo and Honolulu (SSH_{av}) displayed temporal trends in accordance with the 1997–1998 ENSO changes (Figure 1b). High SSH_{av} (strongly positive anomalies) occurred during the 1991–1994 ENSO (SSH_{diff} anomalies > 1). SSH_{av} anomalies became positive between 1995–1996 out of phase with the ENSO cold event, but they became negative during the 1997–1998 strong ENSO warm event. SSH_{av} remained negative following this latter event as the strong ENSO cold event developed; SSH_{av} became positive during 2001–2002 in phase with changes of the ENSO and PDO index. Based on these results, the HOT program biogeochemical data were subsequently divided into five periods: (i) 1989–1990 (ENSO, PDO anomalies weak, variable between -1 and $+1$ and out of phase), (ii) 1991–1994 (ENSO, PDO anomalies $> +1$ and in phase), (iii) 1995–1996 (ENSO negative, PDO anomaly positive and out of phase), (iv) 1997–1998 (ENSO and PDO anomalies both strongly positive and in phase) and (v) 1999–2004 (ENSO and PDO anomalies weak, variable between -1 and $+1$ and in phase).

[13] Monthly MLD anomalies at Station ALOHA significantly decreased during the initial two years of the 1991–1994 ENSO, switching phase in the latter part of 1993 (Figure 1c). During the stronger ENSO event, MLD were significantly greater ($p < 0.005$, $n = 23$) than during the 1991–1994 ENSO event (Table 1). Following the 1997–1998 ENSO event, the average MLD increased significantly and became more variable (50 m vs. 66 m, Table 1). The potential density difference ($\sigma_{\theta \text{ diff MLD-MLD+20m}}$) across the base of the mixed layer, calculated as the difference between the mean σ_{θ} in the MLD and the mean σ_{θ} in the MLD + 20 m layer became significantly positive ($p < 0.005$, $n = 45$) during both the 1991–1994 and the 1997–1998 ENSO warm events (Figure 1d). This indicates a weaker resistance to ML deepening (and entrainment of deeper waters) for a given increase in wind speed. A significant decrease ($p < 0.005$, $n = 23$) in $\sigma_{\theta \text{ diff MLD-MLD+20m}}$ was also observed in the period between the two ENSO warm events.

[14] To further understand the stability dynamics of the water column and the link between upper and lower euphotic zone processes, the potential density difference

Figure 1. Temporal variations in physical properties in the NPSG during 1989–2004, as indicated by (a) the ENSO and PDO anomalies, (b) the SSH monthly average anomaly (i.e. z-score as defined in the text) between Hilo and Honolulu, (c) the monthly anomaly of the mixed layer depth (MLD) at Sta. ALOHA, the monthly anomaly of the mean potential density (σ_{θ}) difference between (d) the MLD+20m layer and the mixed layer, and (e) the MLD+20m layer and the 140–160 m layer at Sta. ALOHA. The red line in Figures 1b, 1c, 1d, and 1e represents the 3-point running average. The temporal boundaries for the five periods used in the statistical analysis (based on different ENSO and PDO variations, as defined in the text) are also shown (vertical black lines in Figure 1a). On the x-axis, each tick mark represents January 1 of each year.

Table 1. Ecosystem Variations at Sta. ALOHA During Periods Characterized by Different ENSO and PDO Variations, as Defined in the Text^a

	1989–1990	1991–1994	1995–1996	1997–1998	1999–2004
PP	0.033 ± 0.004 ^a	0.041 ± 0.001 ^b	0.041 ± 0.003 ^b	0.042 ± 0.002 ^b	0.052 ± 0.002 ^c
PP/Chl <i>a</i>	0.0021 ± 0.001 ^a	0.0023 ± 0.0005 ^a	0.0022 ± 0.0006 ^a	0.0022 ± 0.001 ^a	0.0023 ± 0.0003 ^a
PP/Light	0.020 ^a	0.022 ^b	0.025 ^c	0.023 ^b	0.027 ^c
PP _{0–45m}	0.015 ± 0.001 ^a	0.022 ± 0.001 ^{b,c}	0.025 ± 0.001 ^c	0.021 ± 0.001 ^b	0.024 ± 0.001 ^c
PP _{75–125m}	0.0072 ± 0.0006 ^a	0.0065 ± 0.0005 ^a	0.0061 ± 0.0007 ^a	0.0077 ± 0.0006 ^b	0.0082 ± 0.0003 ^b
PP Winter	0.026 ± 0.002 ^a	0.036 ± 0.002 ^b	0.036 ± 0.001 ^b	0.044 ± 0.003 ^c	0.049 ± 0.004 ^c
PP Spring	0.036 ± 0.002 ^a	0.054 ± 0.005 ^b	0.050 ± 0.006 ^b	0.045 ± 0.005 ^b	0.0050 ± 0.002 ^b
PP Summer	0.030 ± 0.005 ^a	0.042 ± 0.002 ^b	0.043 ± 0.002 ^b	0.045 ± 0.004 ^b	0.058 ± 0.004 ^c
PP Fall	0.033 ± 0.001 ^a	0.043 ± 0.001 ^b	0.029 ± 0.004 ^a	0.037 ± 0.004 ^a	0.045 ± 0.002 ^b
<i>Prochlorococcus</i> spp. _{0–45m}	n/a	74 ± 3 ^a	104 ± 4 ^b	96 ± 5 ^c	55 ± 4 ^d
<i>Synechococcus</i> spp. _{0–45m}	n/a	0.66 ± 0.01 ^a	0.84 ± 0.08 ^b	0.94 ± 0.1 ^b	0.81 ± 0.1 ^b
Picoeukaryotes _{0–45m}	n/a	0.24 ± 0.03 ^a	0.31 ± 0.04 ^b	0.44 ± 0.07 ^c	0.48 ± 0.03 ^c
<i>Prochlorococcus</i> spp. _{75–125m}	n/a	57 ± 4 ^a	77 ± 8 ^b	72 ± 6 ^b	60 ± 3 ^a
<i>Synechococcus</i> spp. _{75–125m}	n/a	0.47 ± 0.07 ^a	0.68 ± 0.11 ^b	0.59 ± 0.07 ^{a,b}	0.56 ± 0.05 ^{a,b}
Picoeukaryotes _{75–125m}	n/a	0.46 ± 0.05 ^a	0.42 ± 0.10 ^a	0.61 ± 0.05 ^b	0.54 ± 0.03 ^b
N + N _{0–45m}	475 ± 274 ^a	127 ± 19 ^b	110 ± 23 ^b	40 ± 6 ^c	70 ± 12 ^d
SRP _{0–45m}	4039 ± 430 ^a	2820 ± 284 ^b	3010 ± 440 ^b	1650 ± 180 ^c	2170 ± 150 ^d
N + N _{75–125m}	3547 ± 360 ^a	3880 ± 890 ^a	5416 ± 200 ^b	5366 ± 190 ^b	5972 ± 140 ^c
SRP _{75–125m}	4293 ± 470 ^a	3707 ± 310 ^a	3850 ± 510 ^a	2970 ± 400 ^b	2830 ± 180 ^b
Particulate C flux	0.0040 ± 0.0002 ^a	0.0030 ± 0.0002 ^b	0.0025 ± 0.0001 ^c	0.0030 ± 0.0001 ^b	0.0028 ± 0.0001 ^{b,c}
PC: PN	8.0 ± 0.1 ^a	8.1 ± 0.2 ^a	8.7 ± 0.2 ^b	8.3 ± 0.3 ^a	7.6 ± 0.2 ^c
PC: PP	197 ± 9 ^a	167 ± 5 ^b	206 ± 11 ^a	215 ± 6 ^a	227 ± 5 ^c
PN: PP	24 ± 1 ^a	20 ± 1 ^b	23 ± 2 ^a	25 ± 1 ^a	30 ± 1 ^c
MLD (<i>i</i> , (<i>ii</i>))	55 ± 7 ^a , 34 ± 5 ^a	50 ± 3 ^b , 28 ± 2 ^b	50 ± 2 ^b , 30 ± 2 ^b	56 ± 4 ^a , 35 ± 5 ^a	66 ± 3 ^c , 36 ± 2 ^a
Temperature	24.8 ± 0.2 ^a	24.8 ± 0.2 ^a	25.2 ± 0.3 ^b	24.5 ± 0.2 ^c	24.8 ± 0.2 ^a
N ²	0.0351 ^a	0.0426 ^b	0.0525 ^c	0.0282 ^d	0.0294 ^d

^aValues represent the mean and 1 SD for each period. Units are mol C m⁻² d⁻¹ for PP, mol C mol Chl a⁻¹ d⁻¹ for PP/Chl *a*, mol C mol quanta⁻¹ for PP/Light, 10¹¹ cells m⁻² for flow cytometric measurements, μmol m⁻² for N + N and SRP, mol C m⁻² day⁻¹ for particulate flux, mol:mol for particulate ratio (e.g., PC:PN, . . .), m for MLD (*i* and *ii* refer to the 0.125 surface offset and 0.005 slope difference in σ_θ , respectively, as defined in the text), °C for temperature and rad/s for N² (Brunt-Väisälä frequency). For each variable, common letters (i.e. a, b, . . .) next to values indicate no statistically significant difference between values (ANOVA and t-test, $p < 0.005$).

(σ_θ diff MLD+20m–140:160m) between the MLD+20m layer and the 140–160 m was calculated. The 140–160 m reference layer was chosen because these depths exceed the average depth of the top of the nutricline [Karl *et al.*, 2002], thereby providing a measure of lower euphotic zone stratification and a proxy of the probability of nutrient injection from the lower into the upper euphotic zone. During the 1991–1994 ENSO, the σ_θ diff MLD+20m–140:160m remained negative, but became positive during and following the 1997–1998 ENSO (Figure 1e), implying increased probability of nutrient injection during the 1997–1998 event. The 140–160 m reference layer was chosen because, based on climatological data at Sta. ALOHA, it is deeper than the mean depth of the top of the nutricline [Karl *et al.*, 2002]. This latter difference (σ_θ diff MLD+20m–140:160m) can then be used as a measure of the lower euphotic zone stratification and as a proxy for the probability of nutrient injection from the lower into the upper euphotic zone (i.e. positive σ_θ diff MLD+20m–140:160m indicates a greater probability of an injection event occurring than negative anomalous σ_θ diff MLD+20m–140:160m).

[15] A clear transition in water column stability at Sta. ALOHA occurred following the 1997–1998 ENSO, as indicated by the mixed layer density anomalies, and mixed layer temperatures and salinity variations (Figures 2 and 3). The Brunt-Väisälä frequency (a measure of the ocean buoyancy damping of turbulence) for the upper 100 m increased significantly during the 1991–1994 ENSO, while it signif-

icantly decreased during and after the 1997–1998 ENSO (Table 1). Furthermore, a clear decrease in the buoyancy frequency below the mixed layer occurred during the 1997–1998 ENSO (Figure 3). Buoyancy frequency time-series revealed a deepening of MLD during the 1997–1998 ENSO. Interannual variability in MLD also demonstrated a clear transition from positive to negative values with the onset of the 1997–1998 ENSO and continuing into 1999 (Figure 4). In particular, the winter and fall anomalies for MLD switched sign following the 1997–1998 ENSO (Figures 4a and 4d).

[16] Concomitant with the shift in water column stability, salinity values at Sta. ALOHA also displayed a clear transition following the 1997–1998 ENSO. Near-surface (5 m) salinity anomalies revealed a progressive increase in salinity with the onset of the 1997–1998 ENSO (Figure 5a). The increase in salinity at the onset of the 1997–1998 ENSO/PDO transition was not confined to surface layers of the euphotic zone, as salinities increased ($p < 0.005$, $n = 65$) throughout most of the euphotic zone (Figure 6). These higher values persisted following the 1997–1998 ENSO.

[17] The shift to higher salinity following the 1997–1998 ENSO/PDO transition was temporally associated with a significant decrease in sea surface temperatures at Station ALOHA starting in late 1996 and lasting through 1998 (Figure 5b and Table 1). However, this temperature change was not associated with a significant change in surface heating, as indicated by sea surface PAR anomalies. Surface

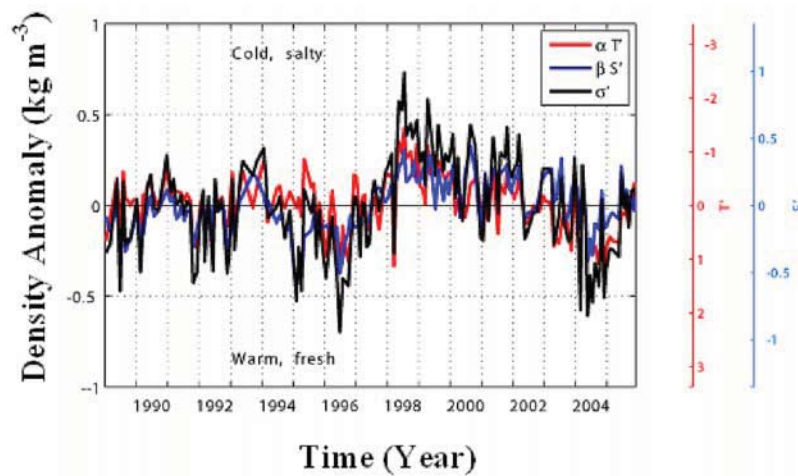


Figure 2. Temporal variations in mixed layer density anomaly (seasonal cycle removed) with the mixed layer temperature and salinity anomalies scaled by their contributions to density at Sta. ALOHA during 1989–2005.

PAR displayed no significant temporal variations (Figure 5c), although strong positive and negative anomalies (i.e. >1 and <-1) were measured in 1992 and 1995, respectively.

3.2. Nutrient Inventories

[18] Nitrate + nitrite ($N + N$) and soluble reactive phosphorus (SRP) concentrations displayed different vertical and temporal trends. In the upper euphotic zone, $N + N_{0-45m}$ anomalies decreased from the beginning of the time-series through 1997–1998 (Figure 7a), with a brief interruption in

1995. Following 1997–1998, $N + N_{0-45m}$ anomalies increased significantly (Figure 7a, $p < 0.005$, $n = 74$). These trends were also confirmed by temporal variations in absolute $N+N$ concentrations between the different ENSO/PDO periods (Table 1). $N + N_{0-45m}$ concentrations were significantly lower during 1997–1998 than at the beginning of the time-series; a small ($30 \mu\text{mol m}^{-2}$), but significant, increase in $N + N_{0-45m}$ concentrations occurred following the 1997–1998 ENSO (Table 1). In the lower euphotic zone, $N + N_{75-125m}$ anomalies remained relatively

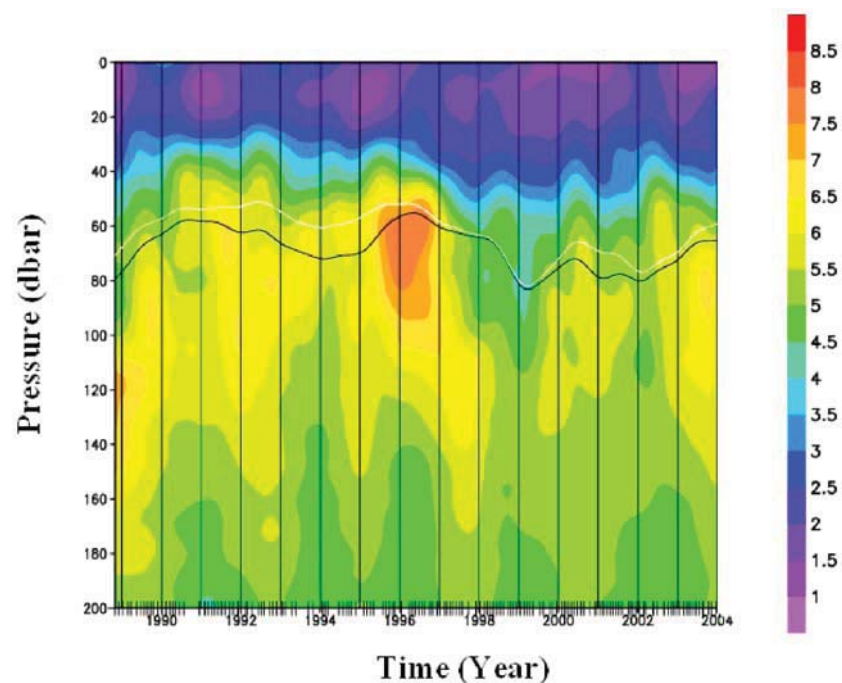


Figure 3. Temporal and vertical variations in the buoyancy frequency (low-pass filtered) at Sta. ALOHA during 1989–2004. Buoyancy frequency units are in cycle hour^{-1} (cph). The black line represents the depth where potential temperature is 0.5°C less than the surface, while the white line represents the depth where σ_θ is 0.125 kg m^{-3} heavier than the surface (i.e. the equivalent density difference if salinity is held constant).

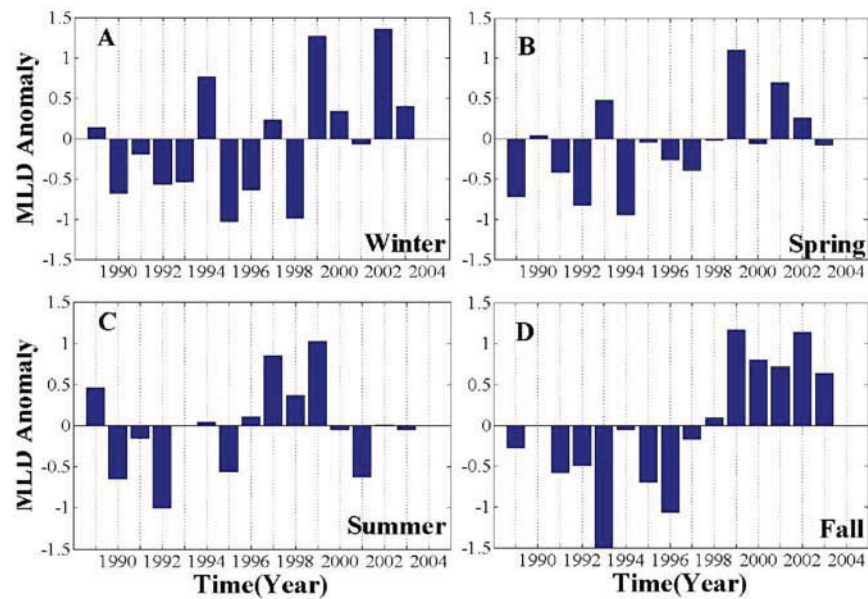


Figure 4. Seasonal variations in MLD (based on 0.125 kg m^{-3} surface offset in σ_θ) anomaly at Sta. ALOHA during 1989–2004. (a) Winter variations include December through February, (b) spring refers to March through May, (c) summer is June through August and (d) fall is September through November.

unchanged, (Figure 7b); however, after 1997–1998, the lower euphotic zone $N + N_{75-125m}$ anomalies were more variable than during the preceding time intervals examined. Absolute $N + N_{75-125m}$ concentrations were also significantly greater following the 1997–1998 ENSO/PDO transition.

[19] Unlike the $N + N_{0-45m}$ anomalies, SRP_{0-45m} anomalies remained relatively unchanged (Figure 7c). However, absolute SRP_{0-45m} concentrations were significantly lower through the 1997–1998 ENSO/PDO transition than at the beginning of the time-series (Table 1). In the lower euphotic zone, $SRP_{75-125m}$ anomalies decreased through the time-series (Figure 7d). Similarly, absolute $SRP_{75-125m}$ concentrations significantly decreased between each consecutive ENSO-PDO period (Table 1).

3.3. Primary Productivity

[20] Rates of primary production (PP) increased significantly throughout the entire 17-year observation period (1989–2004), as shown by significant increases in the monthly anomalies (Figure 8a, $p < 0.005$, $n = 166$), with the greatest increase in PP observed between 1999–2004. The increase in rates of PP was also reflected in differences in the absolute rates of PP measured between 1989–1990 and 1999–2004 (0.033 ± 0.004 vs. $0.052 \pm 0.002 \text{ mol C m}^{-2} \text{ d}^{-1}$, respectively) (Table 1). Interannual dynamics in PP appear characterized by a step function, with stepwise increases observed between 1990–1991 and again between 1997–1998 (Figure 8a). Following both these step increases, PP remained higher than before (Table 1). PP increased by $\sim 0.008 \text{ mol C m}^{-2} \text{ d}^{-1}$ (equivalent to approximately 25%) with the onset of the 1991–1994 ENSO, but remained relatively constant during the onset of the 1997–1998 ENSO/PDO transitions (Figure 8). PP further increased (approximately $0.010 \text{ mol C m}^{-2} \text{ d}^{-1}$ or 30%) after 1997–1998, with large increases observed from mid-1999 to the beginning of 2002.

[21] The monthly anomalies in PP normalized to Chl *a* (PP/Chl *a*) did not show a significant temporal trend (Figure 8b, $p < 0.005$, $n = 166$). This pattern was also reflected in the grouped PP/Chl *a* values (Table 1), where no

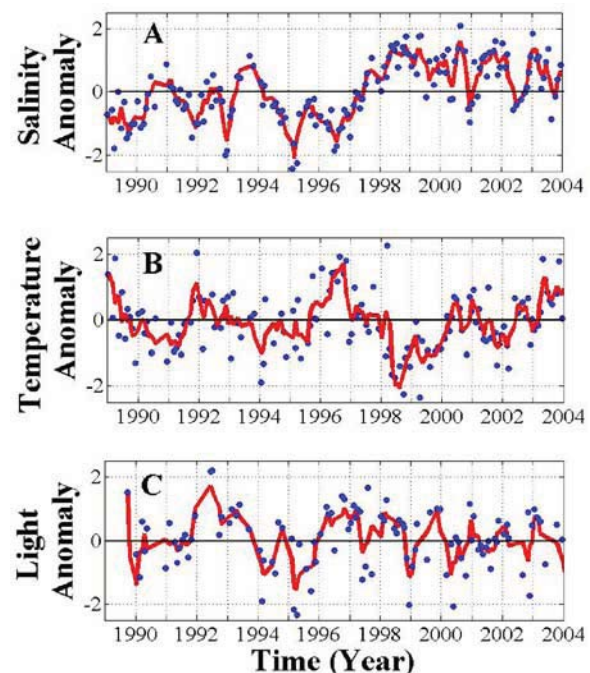


Figure 5. Temporal variations for (a) salinity, (b) temperature and (c) surface PAR anomaly in near-surface waters at Sta. ALOHA. The salinity and temperature records are from 5 m depth at Sta. ALOHA, while the light is the sea surface PAR measured by a Licor meter on deck. The red line in each panel represents the 3-point running average.

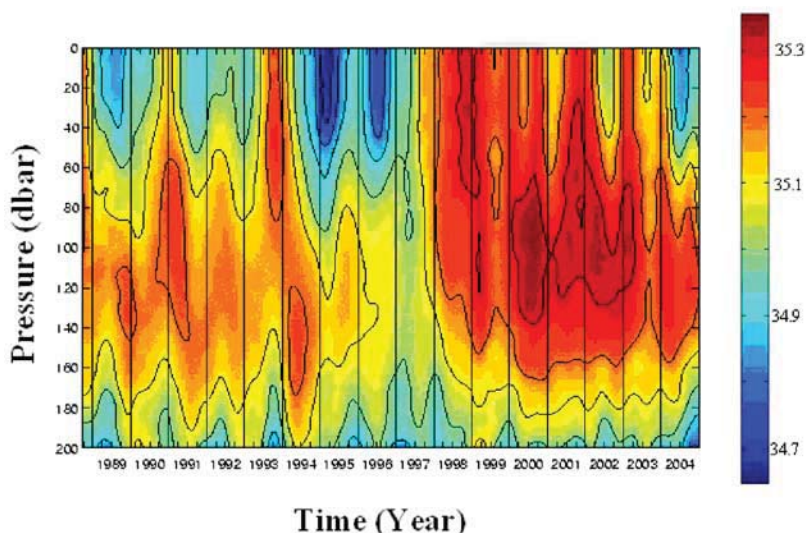


Figure 6. Temporal and vertical variability in salinity in the upper water column (surface to 200 m) at Sta. ALOHA during the 1989–2004 period. Salinity units are in practical salinity units (psu).

significant differences were observed between the different time periods. Anomalies for PP normalized to incident light flux (PP/Light, a proxy for the photosynthetic quantum yield) displayed a significant increase throughout the observation period (Figure 8c, $p < 0.005$, $n = 166$). In addition, PP/Light increased significantly during the 1997–1998 ENSO/PDO transitions (0.020 vs. 0.027 mol C mol quanta⁻¹, respectively) (Table 1).

[22] The observed temporal changes in PP varied between the upper (PP_{0–45m}) and the lower (PP_{75–125m}) euphotic zone, as indicated by seasonal PP anomalies and changes in the depth-integrated rates of PP (Figure 9 and Table 1, respectively). Depth-integrated PP_{0–45m} was higher by

~50% coincident with the 1991–1994 ENSO (Figure 9b, or approximately 0.007 mol C m⁻² d⁻¹, $p < 0.005$, $n = 48$), but was lower by ~15% during the 1997–1998 ENSO/PDO transitions (approximately 0.004 mol C m⁻² d⁻¹, $p < 0.005$, $n = 23$). Conversely, PP_{75–125m} remained constant during the 1991–1994 ENSO, but higher by ~30% (an increase of approximately 0.016 mol C m⁻² d⁻¹) during and following the 1997–1998 ENSO/PDO transitions (Figure 9c and Table 1).

[23] Increases in PP were further demonstrated by comparing seasonal variations in PP (Figure 10 and Table 1). Winter, summer and fall anomalies in PP all showed a clear and significant increase (Table 1) during the 1997–1998

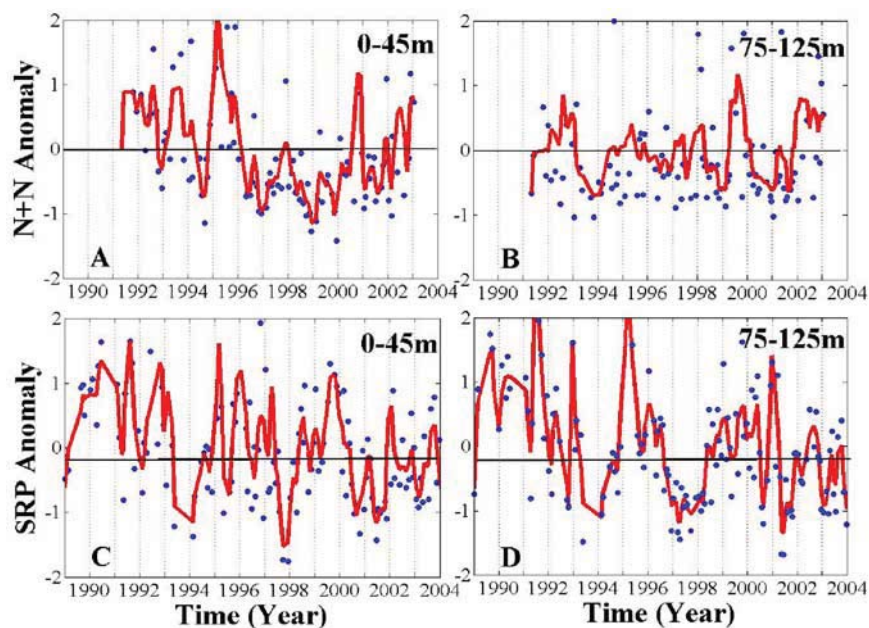


Figure 7. Temporal variations in nitrogen (N + N) and phosphorous (SRP) concentrations in the upper (0–45 m) (a and b, respectively) and lower (75–125 m) (c and d, respectively) euphotic zone at Sta. ALOHA. The red line in each panel represents the 3-point running average.

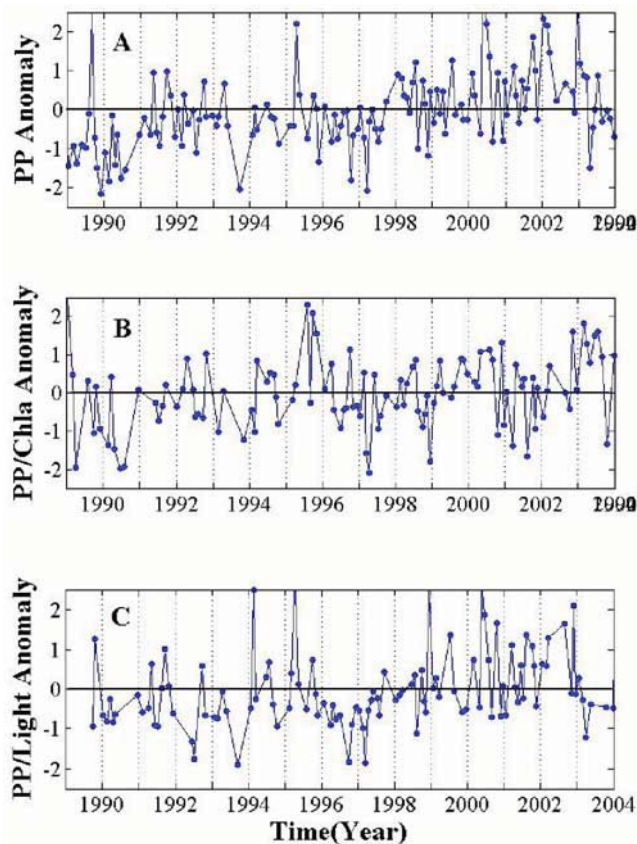


Figure 8. Temporal variations in integrated (a) PP_{0-125m} , (b) $PP/Chl a$ and (c) $PP/Light$ anomaly at Sta. ALOHA during 1989–2004. The $PP/Chl a$ was calculated as depth integrated (0–125 m) PP and $Chl a$, respectively. The $PP/Light$ was calculated based on PP at 5 m depth and surface PAR flux with adjustments for seasonally dependent changes in light extinction coefficients.

ENSO/PDO transition (Figures 10a, 10c, and 10d). Following the 1997–1998 ENSO/PDO transition, summer and fall rates of PP significantly increased (Table 1). The step function increase in PP was also apparent in the winter and summer seasonally binned data (Table 1). Rates of PP in the spring increased by $\sim 50\%$ during the 1991–1994 ENSO, but did not show any other significant variations for the remaining periods examined. During the fall months, PP increased during the 1991–1994 and 1997–1998 ENSO by $\sim 30\%$.

3.4. Planktonic Community Structure and Pigments

[24] Flow cytometric analyses revealed temporal variability in the abundances of the major photoautotrophic groups at Sta. ALOHA following the 1997–1998 ENSO event (Figure 11). The flow cytometric analyses are not available for the initial phase of HOT, including the period before the 1991–1994 ENSO event. In the upper euphotic zone, *Prochlorococcus* spp. concentrations decreased significantly ($p < 0.005$, $n = 83$) following the 1997–1998 ENSO (Figure 11a and Table 1). *Synechococcus* spp. did not display any coherent temporal dynamics (Figure 11c and Table 1). In contrast, picoeukaryote abundances increased during the initial part of the 1997–1998 ENSO

(Figure 11e and Table 1), and continued to significantly increase (Table 1).

[25] In the lower euphotic zone, *Prochlorococcus* spp. cell abundances were temporally variable (Figure 11b), but overall the abundance of *Prochlorococcus* spp. decreased significantly following the 1997–1998 ENSO/PDO transitions (Table 1). In contrast, picoeukaryote abundances increased by 50% during the same time period (Table 1).

[26] Selected pigments, including chlorophyll *b* ($Chl b$, a biomarker for prochlorophytes), 19'-hexanoyloxyfucoxanthin (19'-Hex, a biomarker for prymnesiophytes) and zeaxanthin (Zea, a biomarker for cyanobacteria) [Mackey *et al.*, 1996], were used to evaluate variability in photosynthetic planktonic community structure. With the exception of lower euphotic zone $Chl b$ (Figure 12b), concentrations of all other pigments increased significantly ($p < 0.005$, $n = 850$) following the 1997–1998 ENSO/PDO transition, but remained unchanged during the 1991–1994 ENSO event (Figure 12).

4. Discussion

[27] The connectivity between marine ecosystems and climate variability is thought to depend in part on the

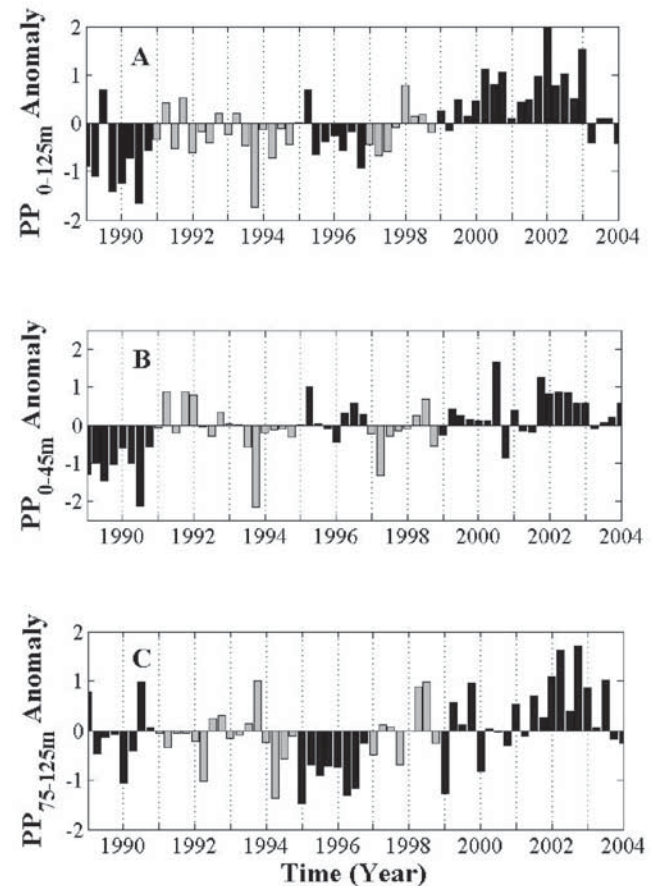


Figure 9. Temporal variations in PP anomaly at Sta. ALOHA during 1989–2004 in (a) the surface to 125 m layer, (b) the upper and (c) lower euphotic zone. Similar colors indicate the same observation period characterized by different ENSO and PDO variations, as defined in the text.

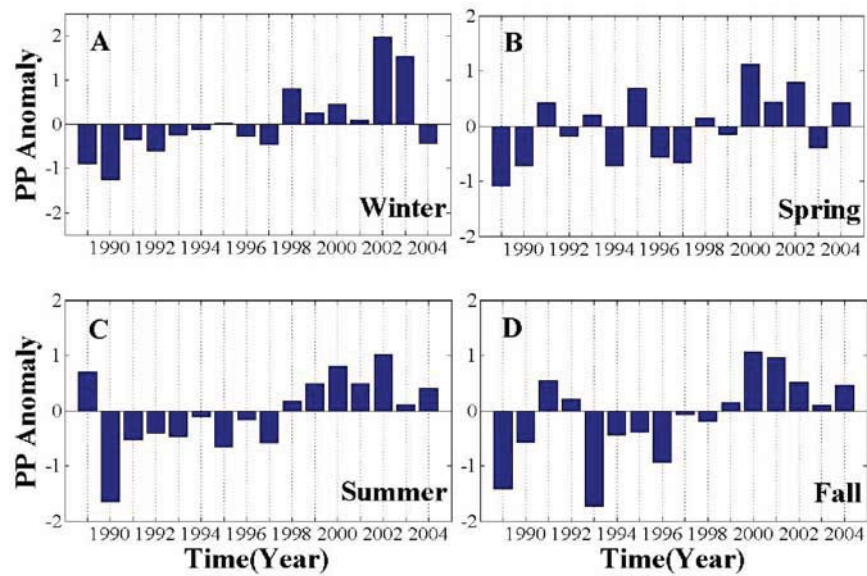


Figure 10. Seasonal anomaly variations in PP at Sta. ALOHA during 1989–2004. Seasonal groupings are the same as for Figure 4.

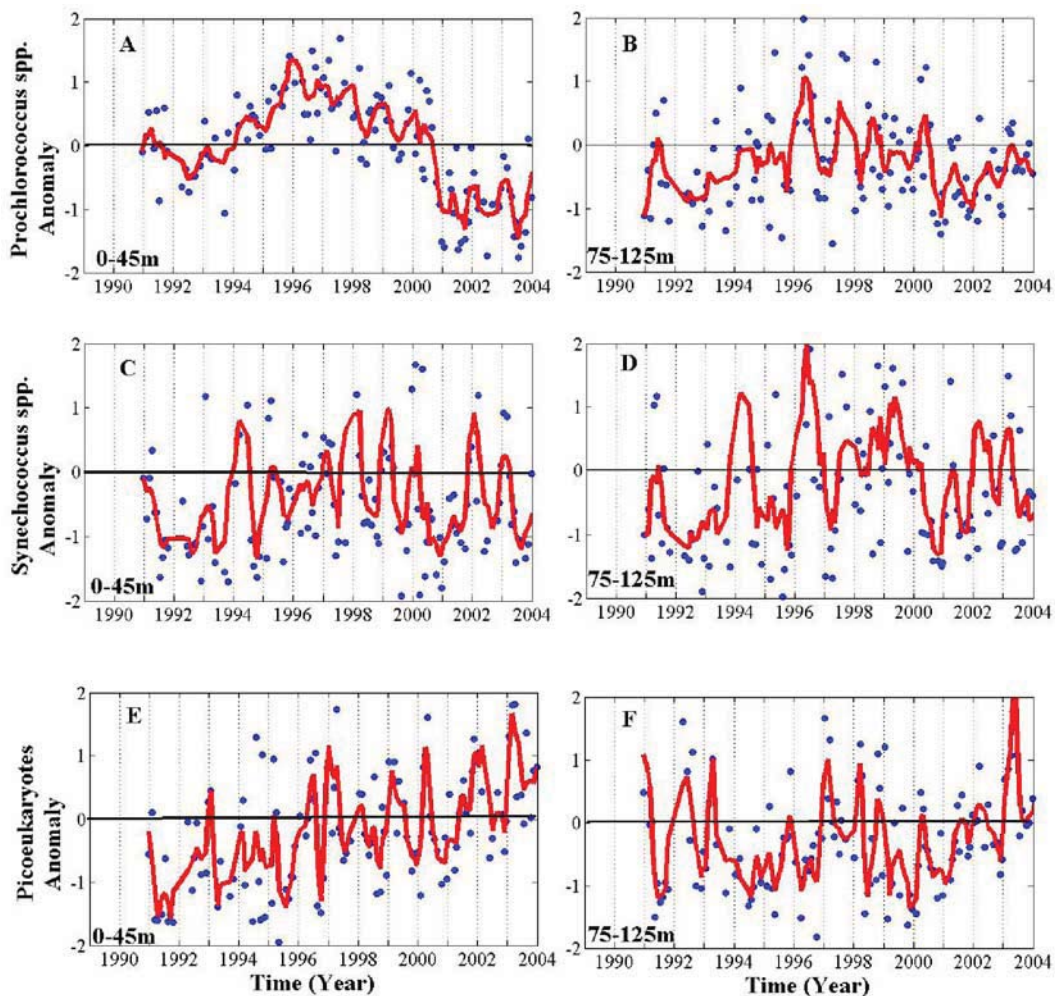


Figure 11. Temporal variations in major photoautotrophs concentrations anomaly at Sta. ALOHA during 1989–2004, based on flow cytometric measurements. Temporal variations for *Prochlorococcus* spp., *Synechococcus* spp. and picoeukaryotes are shown for the upper (a, c, e) and lower (b, d, f) euphotic zone, respectively. The red line in each panel represents the 3-point running average.

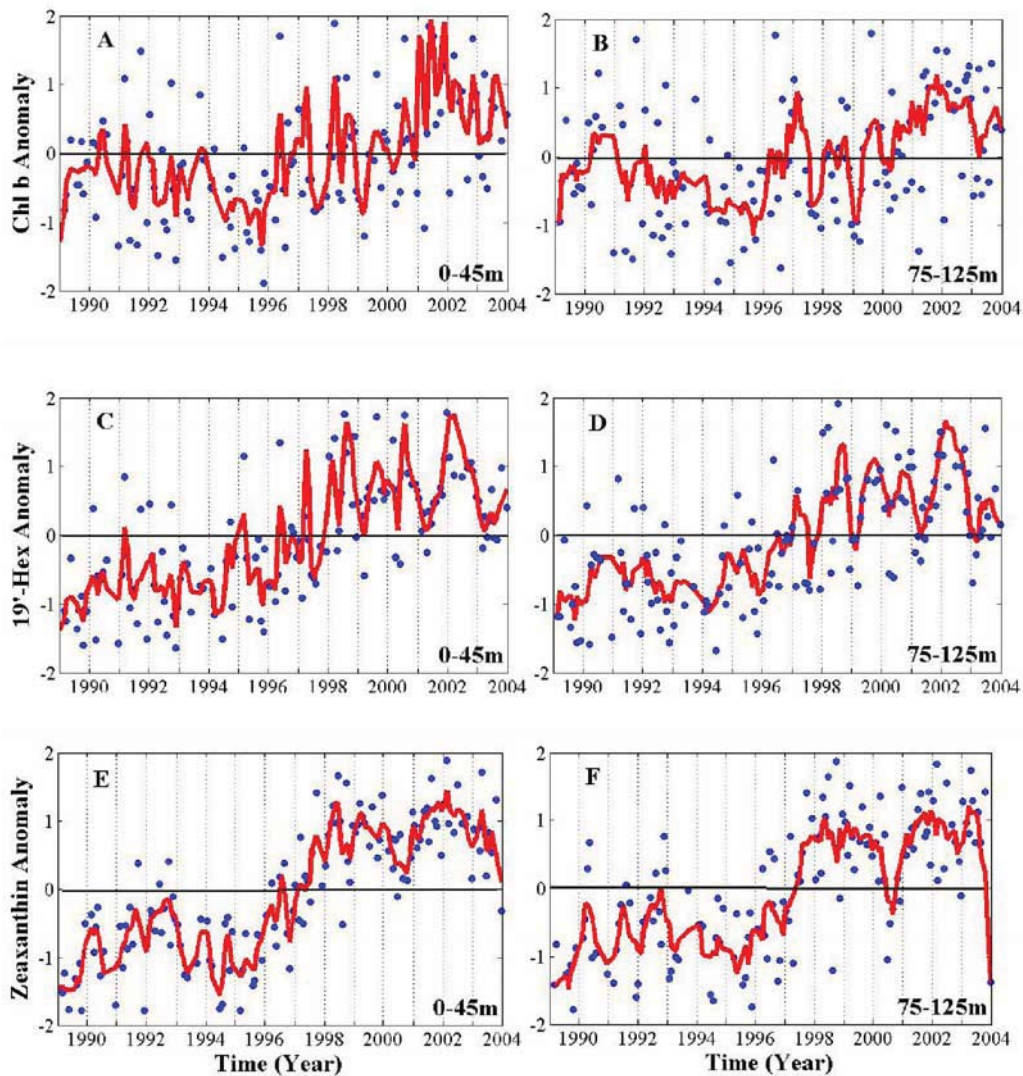


Figure 12. Temporal variations in selected pigment concentrations at Sta. ALOHA during 1989–2004, based on HPLC determination. Pigment concentrations for Chl *b*, 19'-Hex and zeaxanthin are shown for the upper (a, c, e) and lower (b, d, f) euphotic zone, respectively. The red line in each panel represents the 3-point running average.

intensity, duration and frequency of atmospheric forcing of upper ocean physics, including variables such as ocean circulation and stratification. To date, however, we lack clear understanding of the specific relationships that link ocean biota, chemistry, and physics, partly because of the complexity and nonlinearity of marine ecosystems and partly due to the paucity of long-term (decadal scale) data on the time-dependent nature of biogeochemical processes in the sea. Results from the present study suggest that the influences of large-scale, ocean-climate forcing on ecosystem changes can be variable. Such information is of interest when trying to predict future or hindcast past ecosystem changes in relation to climate variability. The different timescales of ENSO and PDO likely confound direct relationships and, in the case of decade-scale phenomena like the PDO, the 17 years of observations at Station ALOHA are not long enough to identify possible relationships between PDO and ecosystem variables. However, the statistical correlation between these two climate drivers of

ocean variability may be useful to predict NPSG ecosystem changes.

[28] Based on analyses of more than 17 years of data on physical, chemical, and biological variability at Sta. ALOHA, the ecosystem's response to two ENSO events did not appear to be consistent, which may be due to a phase reversal in the PDO. When the statistical correlation between the PDO and ENSO events was weakly positive (i.e., they were out of phase, during the 1991–1994 ENSO, $r^2_{\text{ENSO-PDO}} = 0.15$, $p < 0.005$, $n = 48$), rates of PP increased, and the ecosystem appeared to have returned to pre-perturbation conditions. When the statistical correlation between the two indices was strongly positive (i.e., they were in phase during the 1997–1998 ENSO; $r^2_{\text{ENSO-PDO}} = 0.70$, $p < 0.005$, $n = 24$), both rates of PP and export increased. The unique responses of the NPSG ecosystem to combined variability in PDO and ENSO suggest that the response of the upper ocean may be sensitive to competing physical perturbations from both of these ocean-climate

processes. The large-scale physical interaction during these two climate signals appears to influence the wind forcing, heat and fresh water fluxes at the local scale and the ocean-basin scale, and they in turn determine the variation of upper ocean physical properties. During ENSO warm events, when ENSO and PDO signals were not in phase, the trade winds weakened, increasing the stratification of the upper ocean [Karl *et al.*, 1995]. On the other hand, when ENSO and PDO were highly correlated, subsurface water mass changes appear to decrease the upper water column stability.

[29] The issue of delayed ENSO subsurface forcing (via Rossby waves) should also be considered when trying to understand the complexity of the ecosystem-climate relationship. The ecosystem response at ALOHA to direct surface forcing from one ENSO warm event may depend critically on its phasing relative to the delayed subsurface remote forcing from a previous event. It may take 2–3 years for the ENSO Rossby waves to reach Sta. ALOHA after a warm ENSO event gets underway. The mature phase surface forcing will be about 6–9 months after the very beginning of the event onset, so the maximum Rossby wave influence will lag the peak surface forcing by 1.5–2.5 years. In addition to the intensity differences among ENSO warm (and cold) events, there are anomaly pattern differences as well that should be considered. While there is a “canonical” ENSO warm (and cold) event, the actual anomalous atmospheric forcing around Hawaii differs from one event to another [Ropelewski and Halpert, 1987, 1996]. Some, but certainly not all, of these event-to-event differences are due to the PDO [Lukas, 2001; Chu and Chen, 2005].

4.1. Relation of Local Physical Forcing at Sta. ALOHA to ENSO and PDO

[30] Changes in MLD and in the stratification of the lower euphotic zone were critical in influencing PP at Sta. ALOHA, likely as a consequence of changes in light and nutrient availability in the euphotic zone. These variations can be linked to large-scale physical interactions occurring during ENSO and PDO variations. The shoaling of the MLD and stabilization of the upper water column (decrease in N^2) between 1991–1992 appear driven by overall weakening of the trade winds during this period [Karl *et al.*, 1995]. The decrease in upper euphotic zone stability in 1997–1998, when the ENSO index began to increase and, simultaneously, the PDO index displays a sign reversal, could be related to the large-scale shift in surface forcing in the North Pacific occurring at the same time [Lukas, 2001; Keeling *et al.*, 2004]. Sta. ALOHA was within a region of reduced SST (as indicated by the decrease in SST at Sta. ALOHA, Figure 5) and increased northerly and northeasterly winds, resulting in larger variability and increases in the absolute depth of the MLD at Sta. ALOHA. Subduction of anomalous mid-latitude surface water masses and advection by the mean flow of the gyre can also qualitatively account for the upper pycnocline water mass changes [Lukas, 2001]. Together, these processes could explain the reduced stability of the upper ocean at Sta. ALOHA leading to the observed changes in ecosystem structure and function.

[31] The stability decrease of the euphotic zone at Sta. ALOHA following the 1997–1998 ENSO and PDO reversal was clearly indicated by the transition to positive $\sigma_{\theta \text{ diff}}$ anomalies and smaller N^2 absolute values. In particular, the

stability of the lower euphotic zone showed a well-defined reduction during and following the 1997–1998 ENSO and PDO reversal (Figures 1e and 3). During this period, the concomitant decreased stability in the higher and lower euphotic zone most likely increased the probability of surface waters being mixed deeper. During the 1991–1994 ENSO, this simultaneous reduction in stability of the upper and lower euphotic zone did not occur. The reduced stability following the 1997–1998 ENSO stemmed from both increased surface salinities and decreased temperatures, causing an increase in surface density, thus increasing the average MLD. The surface salinity change largely resulted from temporal imbalances in precipitation and evaporation across this region [Lukas, 2001; Dore *et al.*, 2003]. The salinity increase observed below the mixed layer and throughout the euphotic zone may reflect waters that were remotely affected by anomalous surface freshwater fluxes and subsequently subducted and advected to Sta. ALOHA [Lukas, 2001; Keeling *et al.*, 2004]. These physical processes resulted in greater MLD and reduced water column stability at Sta. ALOHA (Table 1). Deep mixed-layers result in lower mean irradiances for the planktonic assemblages in the near surface, and hence lower energy fluxes.

4.2. Variations in PP and Ecosystem States

[32] Similar to changes in the physical stability of the upper ocean, unique responses in measured rates of PP developed during the two ENSO events and PDO phase reversals. The increase in PP during the 1991–1994 ENSO (when the PDO index was in positive phase) has previously been related to an enhancement of N_2 -fixation, caused by a shoaling of the MLD and increased upper ocean stability [Karl *et al.*, 1995]. The increase in PP following the 1997–1998 ENSO and coincident reversal in the PDO likely reflects introduction of new nutrients from across the base of the nutricline due to reduced stratification (decrease in $\sigma_{\theta \text{ diff}}$, lower N^2) of the upper-ocean and increased mixing. The small but significant increase observed in $N + N$ in the upper euphotic zone (Table 1) and the increase in $N + N$ variability in the lower euphotic zone (Figure 7b) after the 1997–1998 ENSO supports this hypothesis. The increased frequency in $N + N$ variability also highlights the role of aperiodic high concentration $N + N$ bursts in alleviating surface nutrient limitation for this ecosystem. Conversely, the observed decrease in soluble reactive phosphorus through the time-series, despite the hypothesized increase in nutrient diffusion following the 1997–1998 ENSO and PDO reversal, may reflect a condition of microbial biomass being perturbed enough to alter the net uptake rates (i.e. uptake \gg regeneration). During the first half of the 1997–1998 ENSO event (spring–fall 1997) PP remained relatively stable despite increasing frequency of $N + N$ spikes. The apparent reasons for the biogeochemical responses to physical forcing during the ENSO and PDO reversals are unknown. However, these upper ocean transitions were accompanied by changes in both the integrated mean light regime and accompanying decrease in the average temperature of the upper ocean, either of which may have decreased phytoplankton growth rates and, therefore, PP.

[33] The observed depth-dependent changes in PP during the two ENSO events supports the hypothesis that N_2 fixation supports a larger fraction of the total production

during the 1991–1994 ENSO event, with NO_3^- -based production accounting for a larger fraction of PP during the 1997–1998 ENSO. Conversely, in the lower euphotic zone, PP increased only during the 1997–1998 ENSO and coincident reversal in the PDO. This observation is consistent with the hypothesis that the source of the new nutrients to the upper ocean derived from increased entrainment across the top of the nitracline.

[34] The variable response in particulate matter flux during the two ENSO events also provides insight into the different biogeochemical responses of climate forcing. Particulate carbon (PC) export decreased during the 1991–1994 ENSO, and increased during the 1997–1998 event (Table 1). The decrease in export could reflect increased retention of organic matter and enhanced re-mineralization in the upper euphotic zone stemming from increased stratification between the mixed-layer and the lower euphotic zone. During the 1997–1998 ENSO event and coincident with the PDO reversal, the disruption of water column stability and subsequent increase in mixing may have enhanced organic material export and provided a mechanism for a greater fraction of the organic matter produced in the euphotic zone to escape re-mineralization and sink deeper in the water column. Biological mechanisms should also be considered as potential explanations for the difference in export during the two ENSO events. Changes in photoautotrophic community structure (as found here with increasing picoeukaryote numbers) towards large cells (therefore more susceptible to sinking) and variations in grazing rates could have led to increased export during the 1997–1998 ENSO. In addition, the inverse relationship between prymnesiophytes concentrations and PC flux following the 1997–1998 ENSO, further supports the hypothesis that a shift in plankton community structure likely altered particulate matter fluxes out of the upper ocean. Such results are in agreement with findings in a different open ocean system [Lomas and Bates, 2004].

[35] Despite the observed variations in PP, the overall nutrient status of photoautotrophic assemblage, as indicated by PP/Chl *a*, appeared temporally stable. PP/Chl *a* can be related to the photosynthetic assimilation number, or productivity index, which represents a proxy for the physiological status of the photoautotrophic community under *situ* conditions. If the PP/Chl *a* is interpreted as evidence for nutrient (usually N) limitation [Karl *et al.*, 2001], then the overall increase in PP and increased nutrient entrainment with the onset of the 1997–1998 ENSO and reversal of the PDO did not appear to alter the underlying physiological nutrient condition of photoautotrophs. Even though some limitations exist regarding the validity of using PP/Chl *a* as a nutrient proxy [Cullen, 1995], this result suggests that (i) greater concentrations of nutrients over longer time periods are needed to significantly affect photoautotrophic physiology in the NPSG, (ii) light limitation, due to increasing mixing, is the main factor influencing the PP/Chl *a*, or (iii) the observed changes in plankton assemblage composition or nutrient uptake rates may have masked apparent changes due to nutrient enrichment.

[36] The change in PP/Light (a proxy for the photosynthetic quantum yield) after the 1997–1998 ENSO suggests an overall increase in the efficiency of light utilization by upper ocean photoautotrophic assemblages. Increases in PP/

Light may have derived from a response by the photoautotrophic community to lower light availability stemming from increased mixing. The combination of various factors, including (i) increased nutrient injection, (ii) variations in light utilization efficiency and (iii) alteration of plankton assemblage composition, all may have contributed to the observed changes in PP following the 1997–1998 ENSO and PDO reversal in 1998.

4.3. Community Structure Changes

[37] The observed variations in physical stability in the euphotic zone of the NPSG also appear to have led to a change in the composition of the photoautotrophic plankton assemblage. Changes in concentrations of *Prochlorococcus* spp., picoeukaryotes and prymnesiophytes (as indicated by $19'$ -Hex concentrations) during and after the 1997–1998 ENSO agree with the hypothesized increase in NO_3^- fluxes from the lower euphotic zone. The recently completed genome sequences of three strains of *Prochlorococcus* spp. highlight that these strains lack the nitrate reductase operon required for NO_3^- utilization [Moore *et al.*, 2002; Dufresne *et al.*, 2003; Rocap *et al.*, 2003]. Decreasing concentrations of surface *Prochlorococcus* spp. abundances following the 1997–1998 ENSO and coincident phase reversal of the PDO may reflect the inability of surface *Prochlorococcus* spp. to compete with other groups of photoautotrophic plankton capable of nitrate utilization, including *Synechococcus* spp. and various groups of picoeukaryotes. In addition, the growth of various strains of *Prochlorococcus* spp. appear sensitive to changes in temperature [Moore *et al.*, 1995; Johnson *et al.*, 2006], suggesting that cooling of the upper ocean following the 1997–1998 ENSO and PDO phase reversal may have allowed photoautotrophic organisms less sensitive to temperature to out-compete *Prochlorococcus* spp.

[38] In the upper euphotic zone, the concomitant increase in Chl *b* and decrease in *Prochlorococcus* spp. are in agreement with the hypothesized increase in mixing and consequent decrease in integrated light availability following the 1997–1998 ENSO. The increase in the ratio Chl *b*: *Prochlorococcus* spp. can be interpreted as a photo-adaptation response to lower light, resulting in a high Chl *b* cell quota. As Chl *b* is the primary accessory pigment in prochlorophytes, increased Chl *b* per cell would enhance the capture of light and energy transfer towards Chl *a* in order to maintain the photosynthetic processes balanced as a response to reduced light availability. Likewise, the increase in zeaxanthin in the lower euphotic zone following the 1997–1998 ENSO could be related to changes in water column stability and light availability. In this context, cyanobacteria populations in the lower euphotic zone would have been subjected to higher light availability (due to increased mixing) following the 1997–1998 ENSO. The relative increase of zeaxanthin per cyanobacterial cell can then be interpreted as a photo-protective process. A higher concentration of zeaxanthin per cell would have protected the photosynthetic apparatus from the increased light availability by dissipating the excess energy in the form of heat and fluorescence through increased rates in the xanthophyll cycle (i.e. increase in zeaxanthin concentrations). Because light availability scales as an exponential of depth, small changes in MLD can lead to large changes in average light.

If light is a major influence on plankton rate processes, then standard ^{14}C in situ (fixed depth) incubations may not accurately estimate primary production. In the upper euphotic zone, the increase in zeaxanthin concentrations following the 1997–1998 ENSO is, however, not yet well understood. In this case, a photo-protective process could not be invoked to explain such change in pigment concentration. Rather than be related to a photo-physiological process, this zeaxanthin increase may well indicate an increase in cyanobacteria species, other than *Prochlorococcus* and *Synechococcus* spp., able to exploit the changed physical and chemical environment following the 1997–1998 ENSO.

[39] The observed increases in the abundances of picoeukaryotes and prymnesiophytes may reflect the ability of these broadly defined groups of pigmented picoplankton to grow on NO_3^- . *Synechococcus* spp. concentrations did not show any particular temporal variations. The unchanged concentrations in the upper euphotic zone during the 1997–1998 ENSO indicates that this organism may well be suited for the hypothesized increase in NO_3^- fluxes in this environment, as shown by the genetic capacity of *Synechococcus* spp. for NO_3^- -based growth [Glover *et al.*, 1988; Moore *et al.*, 2002]. Together, these observations suggest picoeukaryotes and prymnesiophytes may be better adapted to a physically dynamic environment, where temperatures are lower and NO_3^- more readily available. In contrast, during periods of prolonged stability, *Prochlorococcus* spp. abundances increased, likely reflecting the adaptation of these cells to stratified, oligotrophic environments. This is consistent with the domain shift hypothesis and long term changes in the composition of planktonic assembles [Karl *et al.*, 2001].

5. Conclusion

[40] Following nearly two decades of monthly observations at Sta. ALOHA, rates of ^{14}C -derived PP in the NPSG have increased $\sim 50\%$ (Table 1). The observed increases in PP appear to coincide with changes in upper ocean stratification including alteration to the MLD. Changes in euphotic zone water stability have the potential to influence light availability (by decreasing the daily integrated light in the mixed layer due to increasing mixing) and nutrient dynamics in the upper ocean. These local physical changes may demonstrate larger-scale linkages to ocean-basin climate forcing, such as through atmospheric-oceanic interactions occurring during ENSO and PDO. Throughout the latter seven years of time-series observations (1997–2004), rates of PP and export of carbon from the base of the euphotic zone have increased. Coincident in time with changes in the rates of production and export, the upper ocean appeared to undergo a shift in plankton assemblage composition with the abundance of *Prochlorococcus* spp. decreasing, while picoeukaryotes and prymnesiophytes became more abundant.

[41] The observed variations in PP in the NPSG can significantly affect oceanic nutrient cycling, trophic interactions, and global elemental fluxes. Based on time-series analyses of biogeochemical variability at Sta. ALOHA, we suggest that both PP and carbon export may be influenced by large-scale interactions between the atmosphere and the

ocean, e.g., ENSO and PDO. The nature of the ecosystem response depends on both magnitude and duration of the perturbations, the coherence of multiple independent forcings and the interval between major events. It is then important to determine not only possible ecosystem response but also the ecosystem behavior following perturbation. At Sta. ALOHA based on PP dynamics, vertical variations in ecosystem response (upper vs. lower euphotic zone) add a new perspective to this ecosystem behavior. Future analyses are required to relate these temporal PP changes in the NPSG to resilience and resistance dynamics following perturbation. Such an endeavor will help in understanding if ecosystems tend to evolve to the state most resilient to perturbation [Laws, 2003]. Another important issue to be considered is separating the notion of perturbations from shifts. This distinction depends in part on the intensity and scale of the event and the ecological response. In the context of photoautotrophic ecosystems, what might be a climate perturbation (like the observed PP change following the ENSO-PDO variations) might be perceived as a shift. In order to understand these ecosystem characteristics, long-term ecological research, including observations at Station ALOHA, provides crucial information into the timescales of ocean ecosystem behaviors that occur at different time-scales and in a “hidden present” due to their relative slow response and lag following perturbation [Magnuson, 1990].

[42] **Acknowledgments.** The authors would like to thank the Captains and crew of the many research vessels that have supported the HOT program since 1988. We are indebted to all HOT personnel for expert field and laboratory assistance. Yvette Spitz provided valuable comments to the original manuscript. The present research was supported by NSF grant OCE03-26616 (awarded to D.M.K.), OCE-0117919 and OCE-0327513 (awarded to R.L.), and by a grant from the Gordon and Betty Moore Foundation, Marine Microbiology Initiative (awarded to D.M.K.).

References

- Barnett, T. P., D. W. Pierce, M. Latif, D. Dommenges, and R. Saravanan (1999), Interdecadal interactions between the tropics and midlatitudes in the Pacific basin, *Geophys. Res. Lett.*, *26*, 615–618.
- Chu, P.-S., and H. Chen (2005), Interannual and interdecadal rainfall variations in the Hawaiian Islands, *J. Clim.*, *18*, 4796–4813.
- Cullen, J. J. (1995), Status of the iron hypothesis after the open-ocean enrichment experiment, *Limnol. Oceanogr.*, *40*, 1336–1343.
- Dore, J. E., R. Lukas, D. W. Sadler, and D. M. Karl (2003), Climate-driven changes to the atmospheric CO_2 sink in the subtropical North Pacific Ocean, *Nature*, *424*, 754–757.
- Dufresne, A., et al. (2003), Genome sequence of the cyanobacterium *Prochlorococcus marinus* SS120, a nearly minimal oxyphototrophic genome, *Proc. Natl. Acad. Sci.*, *105*, 10,020–10,025.
- Glover, H. E., B. B. Prézelin, L. Campbell, M. Wyman, and C. Garside (1988), A nitrate-dependent *Synechococcus* bloom in surface Sargasso Sea water, *Nature*, *331*, 161–163.
- Graham, N. E. (1994), Decadal-scale climate variability in the tropical and North Pacific during the 1970s and 1980s: Observations and model results, *Clim. Dyn.*, *10*, 135–162.
- Hochberg, Y. (1988), A sharper Bonferroni procedure for multiple tests of significance, *Biometrika*, *75*, 800–803.
- Johnson, Z. I., E. R. Zinser, A. Coe, N. P. McNulty, E. M. Woodward, and S. W. Chisholm (2006), Niche partitioning among *Prochlorococcus* ecotypes along ocean-scale environmental gradients, *Science*, *311*, 1737–1739.
- Karl, D. M. (1999), A sea of change: Biogeochemical variability in the North Pacific Subtropical Gyre, *Ecosystems*, *2*, 181–214.
- Karl, D. M., and R. Lukas (1996), The Hawaii Ocean Time-series (HOT) program: Background, rationale and field implementation, *Deep Sea Res., Part II*, *43*, 129–156.
- Karl, D. M., R. M. Letelier, D. Hebel, L. Tupas, J. Dore, J. Christian, and C. Winn (1995), Ecosystem changes in the North Pacific Subtropical Gyre attributed to the 1991–92 El-Niño, *Nature*, *373*, 230–234.

- Karl, D. M., D. V. Dore, R. M. Hebel, R. M. Letelier, and L. M. Tupas (1996), Seasonal and interannual variability in primary productivity and particle flux at Station ALOHA, *Deep Sea Res., Part II*, 43, 539–568.
- Karl, D. M., R. R. Bidigare, and R. M. Letelier (2001), Long-term changes in plankton community structure and productivity in the North Pacific Subtropical Gyre: The domain shift hypothesis, *Deep Sea Res., Part II*, 48, 1449–1470.
- Karl, D. M., R. R. Bidigare, and R. M. Letelier (2002), Sustained and aperiodic variability in organic matter production and phototrophic microbial community structure in the North Pacific Subtropical Gyre, in *Phytoplankton Productivity and Carbon Assimilation in Marine and Freshwater Ecosystems*, edited by P. J. le B. Williams, D. R. Thomas, and C. S. Reynolds, pp. 222–264, Blackwell, Malden, Mass.
- Keeling, C. D., H. Brix, and N. Gruber (2004), Seasonal and long-term dynamics of the upper ocean carbon cycle at Station ALOHA near Hawaii, *Global Biogeochem. Cycles*, 18, GB4006, doi:10.1029/2004GB002227.
- Laws, E. A. (2003), Partitioning of microbial biomass in pelagic aquatic communities: Maximum resiliency as a food web organizing construct, *Aquat. Microbiol. Ecol.*, 32, 1–10.
- Laws, E. A., G. R. DiTullio, and D. G. Redalje (1987), High phytoplankton growth and production rates in the North Pacific Subtropical Gyre, *Limnol. Oceanogr.*, 32, 905–918.
- Letelier, R. M., J. E. Dore, C. D. Winn, and D. M. Karl (1996), Seasonal and interannual variations in photosynthetic carbon assimilation at Station ALOHA, *Deep Sea Res., Part II*, 43, 467–487.
- Letelier, R. M., D. M. Karl, M. R. Abbott, P. Flament, M. Freilich, R. Lukas, and T. Strub (2000), Role of late winter mesoscale events in the biogeochemical variability of the upper water column of the North Pacific Subtropical Gyre, *J. Geophys. Res.*, 105, 28,723–28,739.
- Lomas, W., and N. R. Bates (2004), Potential controls on interannual partitioning of organic carbon during the winter spring phytoplankton bloom at the Bermuda Atlantic time-series study (BATS) site, *Deep Sea Res., Part I*, 51, 1619–1636.
- Longhurst, A., S. Sathyendranath, T. Platt, and C. Caverhill (1995), An estimate of global primary production in the ocean from satellite radiometer data, *J. Plankton Res.*, 17, 1245–1271.
- Lukas, R. (2001), Freshening of the upper thermocline in the North Pacific Subtropical Gyre associated with decadal changes of rainfall, *Geophys. Res. Lett.*, 28, 3485–3488.
- Mackey, M. D., D. J. Mackey, H. W. Higgins, and S. W. Wright (1996), CHEMTAX—A program for estimating class abundances from chemical markers: Application to HPLC measurements of phytoplankton, *Mar. Ecol. Prog. Ser.*, 144, 265–283.
- Magnuson, J. J. (1990), Long-term research and the invisible present, *BioScience*, 40, 495–501.
- Mantua, N., S. Hare, Y. Zhang, J. Wallace, and R. Francis (1997), A Pacific interdecadal climate oscillation with impacts on salmon production, *Bull. Am. Meteorol. Soc.*, 78, 1069–1079.
- Marañón, E., M. J. Behrenfeld, N. Gonzalez, B. Mourino, and M. V. Zubkov (2003), High variability of primary production in oligotrophic waters of the Atlantic Ocean: Uncoupling from phytoplankton biomass and size structure, *Mar. Ecol. Prog. Ser.*, 257, 1–11.
- Martin, J. H., G. A. Knauer, D. M. Karl, and W. W. Broenkow (1987), VERTEX: Carbon cycling in the northeast Pacific, *Deep Sea Res., Part I*, 34, 267–285.
- Moore, L. R., R. Goericke, and S. W. Chisholm (1995), Comparative physiology of *Synechococcus* and *Prochlorococcus*: Influence of light and temperature on growth, pigments, fluorescence, and absorptive properties, *Mar. Ecol. Prog. Ser.*, 116, 259–275.
- Moore, L. R., A. F. Post, G. Rocap, and S. W. Chisholm (2002), Utilization of different nitrogen sources by the marine cyanobacteria, *Prochlorococcus* and *Synechococcus*, *Limnol. Oceanogr.*, 47, 989–996.
- Rocap, G., et al. (2003), Genome divergence in two *Prochlorococcus* ecotypes reflects oceanic niche differentiation, *Nature*, 424, 1042–1047.
- Ropelewski, C. F., and M. S. Halpert (1987), Global and regional scale precipitation patterns associated with the El Niño/Southern Oscillation, *Mon. Weather Rev.*, 115, 1606–1626.
- Ropelewski, C. F., and M. S. Halpert (1996), Quantifying Southern Oscillation-precipitation relationships, *J. Clim.*, 9, 1043–1059.
- Sakamoto, C., D. M. Karl, H. W. Jannasch, R. R. Bidigare, R. M. Letelier, P. M. Walz, J. R. Ryan, P. S. Polit, and K. S. Johnson (2004), Influence of Rossby waves on nutrient dynamics and the plankton community structure in the North Pacific Subtropical Gyre, *J. Geophys. Res.*, 109, C05032, doi:10.1029/2003JC001976.
- Venrick, E. L., J. A. McGowan, D. R. Cayan, and T. L. Hayward (1987), Climate and chlorophyll *a*: Long-term trends in the Central North Pacific Ocean, *Science*, 237, 70–72.
- Wilson, C. (2003), Late summer chlorophyll blooms in the oligotrophic North Pacific Subtropical Gyre, *Geophys. Res. Lett.*, 30(18), 1942, doi:10.1029/2003GL017770.
- Wolter, K., and M. S. Timlin (1998), Measuring the strength of ENSO—How does 1997/98 rank?, *Weather*, 53, 315–324.

M. R. Abbott and R. M. Letelier, College of Oceanic and Atmospheric Sciences, Oregon State University, 104 Ocean. Admin. Bldg., Corvallis, OR 97331-5503, USA.

R. R. Bidigare, The Hawaii Institute of Marine Biology, P.O. Box 1346, Kaneohe, HI 96744, USA.

M. J. Church, D. M. Karl, and R. Lukas, School of Ocean and Earth Science and Technology, University of Hawaii, Honolulu, HI 96822, USA.

G. Corno, UNESCO-Quito, Av. Juan León Mera 130 y Av. Patria Ed. CFN 6to. Piso Apartado: 17-07-8998, Quito, Ecuador. (gcorno@unesco.org.ec)